

## Original Article : Open Access

## Green synthesis of gold nanoparticles using neem seed extract: Antioxidant, antimicrobial, and catalytic properties

Rajita Beniwal, Sushila Singh<sup>♦</sup>, Seema Sangwan\*, Ritu Devi, Monika Moond, Jyoti Duhan and Kamaljeet Saini

Department of Chemistry, CCS Haryana Agricultural University, Hisar-125001, Haryana, India

\*Department of Microbiology, CCS Haryana Agricultural University, Hisar-125001, Haryana, India

### Article Info

#### Article history

Received 15 July 2024  
Revised 3 September 2024  
Accepted 4 September 2024  
Published Online 30 December 2024

#### Keywords

Nanotechnology  
Gold nanoparticles  
Green synthesis  
Optimization  
Catalytic  
Antimicrobial

### Abstract

Gold nanoparticles are one of the most distinguished nanoscale metallic materials that have garnered more attention among the various noble metallic nanoparticles with potential applications in catalysis, biotechnology, pharmacology, medical imaging, optics, *etc.*, because of their low toxicity, biocompatibility, and high surface to volume ratio that can be functionalised with various ligands. Due to their medicinal, biological and economic importance, *Azadirachta indica* A. Juss. seeds were selected for the biosynthesis of gold nanoparticles (AuNPs) due to their low cost, one step, eco-friendly and no need for reducing and stabilizing agents. Optimization of various parameters was performed during the biosynthesis of gold nanoparticles, which influenced the size and morphology of the synthesized nanoparticles (NPs). AuNPs' surface plasmon resonance (SPR) was detected between 530 and 550 nm. Characterization of the biosynthesized NPs was performed by using different techniques. Under optimal conditions, the size of the nanoparticles was found to be between 10 and 25 nm. An aqueous extract of the seeds was compared to the antioxidant and antimicrobial (antibacterial and antifungal) properties of gold nanoparticles. The efficient catalytic activity of AuNPs was observed in the first order reduction reaction of 4-nitrophenol to 4-aminophenol with a rate constant of 0.103 min<sup>-1</sup>. The results showed that an efficient, low-cost green method for the biosynthesis of AuNPs using *A. indica* seed aqueous extract, with significant biological and catalytic properties.

### 1. Introduction

Since metal nanoparticles are used in chemistry, medicine, electronics, optics, and pharmaceutical sciences, they can be regarded as one of the most varied types of nanoparticles (Moond *et al.*, 2023; Rani *et al.*, 2024). Chemical, physical, and biological techniques can be used to create and stabilise these metal nanoparticles. The synthesis of nanoparticles by physical and chemical methods has already been widely discussed, but these methods involve the use of non-polar solvents and toxic chemicals, with dangerous environmental impacts and many steps for the purification of product, thus resulting in an expensive route (Khan *et al.*, 2018; Singh *et al.*, 2021). Thus, green chemistry was developed as an alternative to the use of environmentally adverse process and substances due to the serious negative consequences facing the world today and lack of time to find effective solutions for the remediation (Moond *et al.*, 2022; Moond *et al.*, 2023). Today, chemical technologists and chemists use the twelve principles of green chemistry as a standard for creating less dangerous chemical synthesis (Anastas and Warner, 1998; Moond *et al.*, 2023; Poonam *et al.*, 2023; Moond *et al.*, 2024).

Plant bioactive chemicals with high redox potential, such as phenolic acid, flavanoids, citric acid, alkaloids, ascorbic acid, and others, operate as reducing and capping agents (Santosh Kumar *et al.*, 2017; Aggarwal

*et al.*, 2022; Dalal *et al.*, 2022; Devi *et al.*, 2023; Moond *et al.*, 2023). Medicinal plants have long been used to treat and prevent illness all over the world. The most important medicinal plant, *Azadirachta indica* A. Juss. popularly known as Neem, belongs to the Meliaceae family and is regarded as "The Village Pharmacy" because to its healing ability (Beniwal *et al.*, 2023). *A. indica* is also known as 'Aristha,' which means "Srva Roga Nivarini," which translates to "the healer of all ills", "divine tree" and "nature's pharmacy" (Prashanth and Krishnaiah, 2014; Puri, 1999). With more than 140 components extracted from various areas of the plant, *A. indica* contains a wide range of phytochemicals that are chemically and structurally diverse. Many phytochemicals can be extracted from *A. indica*'s chemical constituents, including phenolic compounds, flavanoids, alkaloids, triterpenoids, carotenoids, steroids, limonoides, saladin, nimbolide, margolone, margolonone, isomargolonone, quercetin, gallic acid, salanin, azadirone, nimbinine, nimboline A, nimboline B, valassin, volatile oils, nimbin, nimbicin, geducin and azadirachthin (Singh and Chauhan, 2014; Subapriya and Nagini, 2005) which are used as anti-inflammatory, antipyretic, antibacterial, antigastric ulcer, antimalarial, antiarthritic, antifungal, antitumor and immunomodulatory (Eid *et al.*, 2017).

In the literature, there have been several research on the antioxidant and antibacterial activities of *A. indica* (Sithisarn *et al.*, 2005; Nahak and Sahu 2011; Mahmoud *et al.*, 2011). The utilization of *A. indica* seed aqueous extract in the production of gold nanoparticles was investigated utilizing an environmentally benign and low-cost technique. The impact of various physicochemical parameters (extract concentration, gold salt concentration, temperature, pH, and reaction duration) on biosynthesis of AuNPs and their characterization using

#### Corresponding author: Dr. Sushila Singh

Assistant Professor, Department of Chemistry, CCS Haryana Agricultural University, Hisar-125004, Haryana, India

E-mail: [singhsushila999@gmail.com](mailto:singhsushila999@gmail.com)

Tel.: +91-8199939339

Copyright © 2024 Ukaaz Publications. All rights reserved.

Email: [ukaaz@yahoo.com](mailto:ukaaz@yahoo.com); Website: [www.ukaazpublications.com](http://www.ukaazpublications.com)

various techniques was also investigated. Aqueous seed extract of *A. indica* was compared to biosynthesized gold nanoparticles for biological activities (antioxidant and antibacterial) (AuNPs). The catalytic activity of biosynthesized AuNPs was examined for the reduction of 4-nitrophenol to 4-aminophenol in the presence of an aqueous solution of sodium borohydride ( $\text{NaBH}_4$ ).

## 2. Materials and Methods

### 2.1 Preparation of plant extract

Seeds of *A. indica* were procured from research area, Department of Forestry of CCS HAU, Hisar. Dr. Anita, Assistant Scientist, Department of Botany and Plant Physiology, CCS HAU, by using online platform on Atlas of Florida plants and cited as Mém. Mus. hist. Nat. 19: 221. 1830. A 10 g seed powdered sample was refluxed in 150 ml deionized water for 1 h at  $40^\circ\text{C}$  before being filtered through Whatman No. 1 filter paper. The extract was ready for additional analysis after it was centrifuged for 10 min at 7500 rpm and then run through a microsyringe filter ( $0.25\ \mu\text{m}$ ).

### 2.2 Biosynthesis of AuNPs at optimized conditions

For the biosynthesis of AuNPs, aliquots of *A. indica* seed extracts were added dropwise to the precursor solution ( $\text{HAuCl}_4 \cdot 3\text{H}_2\text{O}$ ) held on magnetic stirrer at 1200 rpm at neutral pH and room temperature in the dark after optimization of various physicochemical parameters. To eliminate any big entities, the reaction mixture was centrifuged at 7500 rpm for 20 min. The supernatant was removed using a pipette, and the sediment was rinsed multiple times with deionized water before being washed with 100% ethanol. Sediment thus obtained was lyophilized to get the powdered *A. indica* seed gold nanoparticles (NS-AuNPs).

### 2.3 Characterization of biosynthesized gold nanoparticles (AuNPs)

The size, form, and morphology of NS-AuNPs were studied in order to characterize them. Particle size analyzer (PSA), UV-Vis spectroscopy, fourier-transform infrared (FT-IR) spectroscopy, high resolution transmission electron microscope (HRTEM), field emission scanning electron microscope (FESEM), and X-ray diffraction were used to characterize the synthesized eco-friendly *A. indica* seeds mediated AuNPs (XRD). The synthesised AuNPs were characterised using UV-Vis spectroscopy. A UV-Vis double beam Spectrophotometer (Model UV 1900, Shimadzu) was used in conjunction with 'Multi Wavelength Professional' computer software to conduct the spectrum scan. The wavelength range of 300-900 nm was used for UV-Vis spectroscopy. In all scans, we utilized distilled  $\text{H}_2\text{O}$  as a blank. Using

the Microtracnanotracs wave II Instrument, the hydrodynamic size distributions, zeta potential, and polydispersity index (PDI) of the nanoparticles were ascertained (PSA). FT-IR spectrophotometer was used to investigate the presence of various functional groups in plant extracts and biosynthesized AuNPs (Perkin Elmer spectrum 3). A field emission scanning electron microscope (FESEM, JSM-7610FPlus) fitted with an energy dispersive X-ray spectroscopy (EDS) detector and operating at an accelerating voltage of 0.1 to 30 kV was used to analyse the surface morphology and elemental mapping of biosynthesised AuNPs. High-resolution morphology, structure, crystallography, and dispersion of nanomaterials are determined by TEM examination. Images were captured using an FEI Technai G2 20 with a 200 kV accelerating voltage.

### 2.4 Antioxidant potential

Total antioxidant capacity (TAC) was assessed using the modified phosphomolybdenum method (Prieto *et al.*, 1999) and the DPPH free radical scavenging method (Hatano *et al.*, 1988) to assess the antioxidant activity of *A. indica* seeds and their biosynthesised nanoparticles.

### 2.5 Study of catalytic activity of synthesized gold nanoparticles (AuNPs)

Gold metallic nanoparticles, which enable electron transfer from  $\text{BH}_4$  to 4-nitrophenol, catalyse the reduction reaction (4-nitrophenol to 4-aminophenol) in the presence of  $\text{NaBH}_4$ . The absorbance of an aqueous solution of 4-nitrophenol (0.01 M,  $40\ \mu\text{l}$ ) was measured after it was diluted to 3 ml with deionized water ( $\lambda_{\text{max}} = 319.4\ \text{nm}$ ). An aliquot of the 4-nitrophenol solution (0.01 M,  $40\ \mu\text{l}$ ) was reacted with freshly made  $\text{NaBH}_4$  solution (0.1 M, 0.2 ml), further diluted to 3 ml with deionized water, and then absorbance was measured ( $\lambda_{\text{max}} = 402\ \text{nm}$ ). Then, independently, another aliquot of 4-nitrophenol solution (0.01M,  $40\ \mu\text{l}$ ) was reacted with freshly generated  $\text{NaBH}_4$  solution (0.1 M, 0.2 ml) and treated with gold nanoparticles (AuNPs) obtained from *A. indica* seed ( $40\ \mu\text{l}$ ). The reaction mixture was thoroughly mixed, and UV-visible spectroscopy was used to track the reaction's development (Dash and Bag, 2014). The kinetic equation can be shown as follows:

$$\ln C_p / C_t = \ln A_0 / A_t$$

By plotting a graph between  $\ln (A/A_0)$  versus time, value of rate constant was obtained. Possible mechanism for reduction of 4-nitrophenol to 4-aminophenol can be explained as Figure 1.

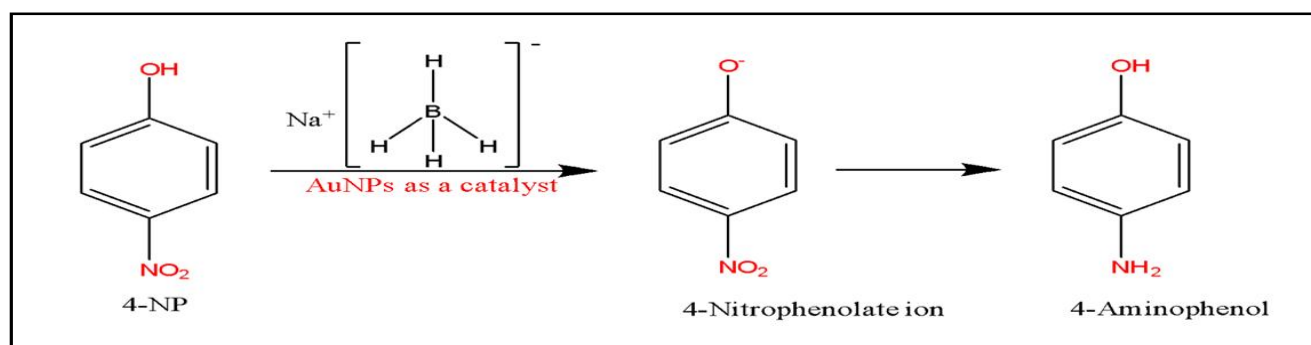


Figure 1: Reduction of 4-NP to 4-aminophenol by using AuNPs as a catalyst.

## 2.6 Evaluation of antimicrobial activity

Antimicrobial experiments using the agar well diffusion technique were performed on Gram-positive *Staphylococcus aureus* and Gram-negative *Xanthomonas species*. All antibacterial investigations employed *Streptomycin* (15 µg/ml) with a 0.5 cm diameter as a positive control. The antifungal activity of the synthesised compounds was evaluated against a fungal strain using the agar well diffusion method, which was supported according to protocol. Antifungal tests were conducted with *Macrophomina phaseolina* and *Fusarium oxysporum*. Nystatin (20 µg/ml) was used as a positive control in all antifungal experiments.

## 3. Results

### 3.1 Biosynthesis, optimized conditions and stability of biosynthesized

AuNPs biosynthesis of AuNPs by using *A. indica* seed extract was done under optimized conditions of 80 µl extract concentration, 1 mM gold salt concentration at room temperature, neutral pH and reaction duration of 120 min. Stability of nanoparticles can be explained on the basis of zeta potential. Value of zeta potential was found to be -39.6 mv for NS-AuNPs. High surface charge on AuNPs prevents their aggregation, so were found to be stable for more than 15 days.

### 3.2 Proposed mechanism of biosynthesis of AuNPs by using *A. indica* seed aqueous extract

Flavanoids have also been linked to the reduction of metal ions to metallic nanoparticles. Flavanoids with a concentration of more than 1.25 mg/ml were shown to reduce gold ions in gold atoms by 95% (Zhou *et al.*, 2010). *A. indica* seed extracts have been discovered to have a high flavonoid concentration, making them a strong reductant for gold nanoparticle production. The number of free -OH and -C=O groups to contribute electrons determines flavanoid's capacity to reduce and stabilize. As a result, a potential reaction mechanism for the biosynthesis of AuNPs based on the use of catechin (flavanoid) as a reducing agent is proposed. Catechin is transformed to semiquinones by losing a hydrogen atom from the -OH group, which are then oxidised to stable quinones. The electrons created during this process decreased gold ions ( $\text{Au}^{+3}$ ) to AuNPs, as illustrated in Figure 2. Quinones then bind to the surface of AuNPs *via* their negatively charged -C=O group, acting as a capping agent to prevent NPs aggregation and improve colloidal stability over time (Ghoreishi *et al.*, 2011). Based on the results of the experiments, a broad hypothetical reaction mechanism was put forth using the seed extract of *A. indica* to explain the function of flavanoids during the synthesis and stabilisation of gold nanoparticles.

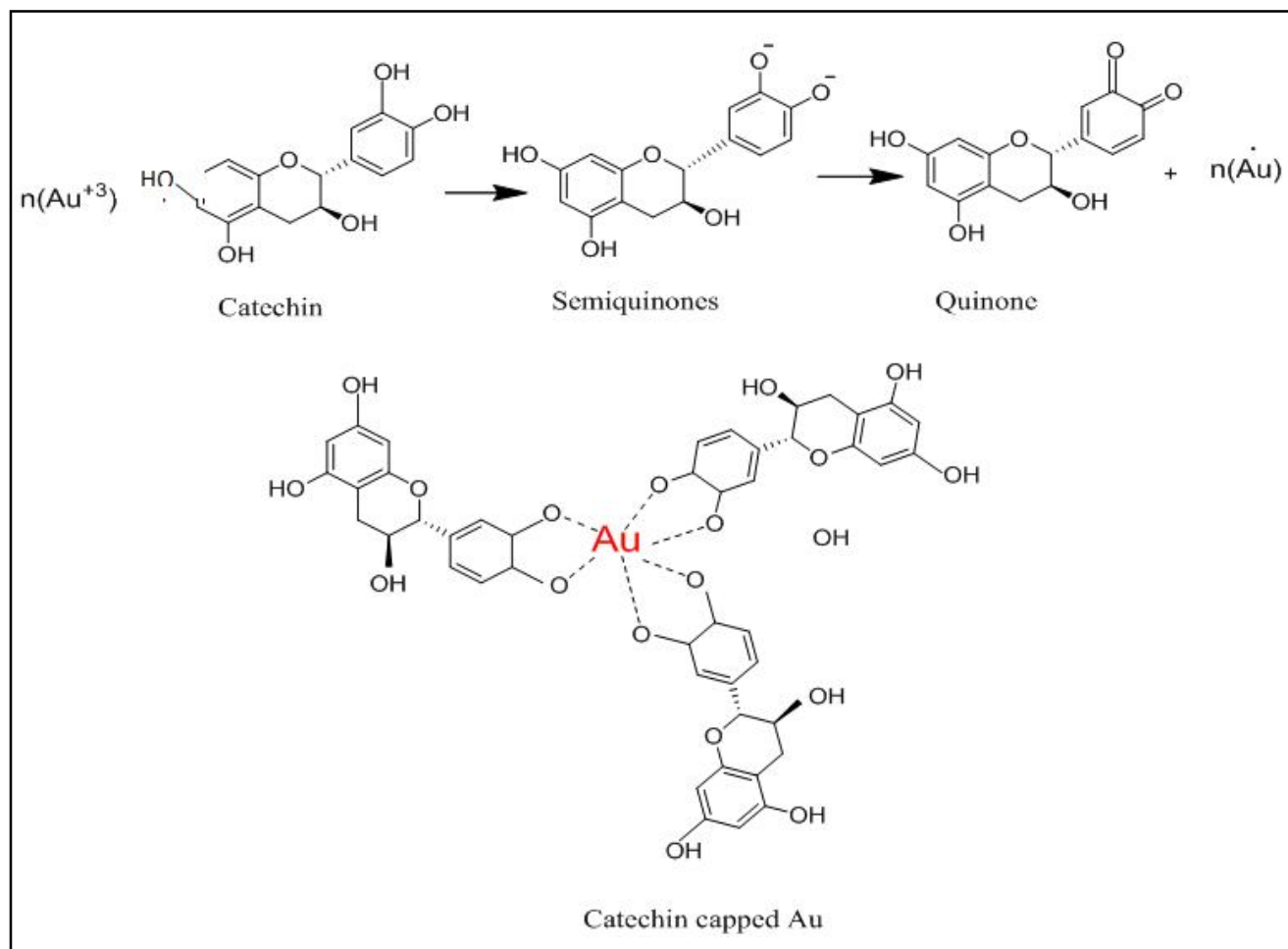


Figure 2: Proposed reduction and stabilization of gold ions with catechin.

From FT-IR data analysis, similarity between extract's peak position and their biosynthesized AuNPs confirmed the presence of bioactive compounds on the surface of NPs. Red shift towards longer wave number ( $3325$  to  $3337\text{ cm}^{-1}$ ) was observed for stretching vibrations of O-H group of phenolics and flavanoids which assured the involvement of O-H group in retention on the surface of AuNPs. On the other hand, blue shift towards shorter wave number was observed for  $\text{-C=O}$  group ( $1652$  to  $1646\text{ cm}^{-1}$ ) indicating the oxidation of hydroxyl to carbonyl group which were adsorbed on the surface of AuNPs through their negatively charged groups and thus prevents aggregation and increased the stability of colloidal system.

### 3.3 Characterization of biosynthesized AuNPs

UV-Vis spectrophotometer was used as preliminary tool for the assessment and determination of several properties of biosynthesized AuNPs. Biosynthesized AuNPs in aqueous solution exhibited strong and intense surface plasmon resonance (SPR) band in between  $500$ - $600\text{ nm}$  (Anuradha *et al.*, 2010; Ismail *et al.*, 2014). The average particle size, zeta potential and polydispersity index (PDI) of biosynthesized NS-AuNPs were found to be  $61.8\text{ nm}$ ,  $-39.6\text{ mv}$  and  $0.14$ , respectively (Figure 3a) (Kumar *et al.*, 2011; Kumar *et al.*,

2016). The crystalline structure and surface morphology of the biosynthesized AuNPs by using *A. indica* seed was identified by X-ray diffraction (XRD) at  $2\theta$  angles in the range of  $10$ - $80^\circ$ . The diffraction peaks of biosynthesized AuNPs by using *A. indica* seed were observed at round  $2\theta = 38.16$ ,  $44.42$ ,  $64.68$  and  $77.6$  which corresponds to (111), (200), (220) and (311) Bragg reflections (Figure 3b), respectively, which were comparable to those reported for the FCC lattice structure of standard gold (Au) metal (JCPDS No. 04-0784) (Gopalakrishnan and Raghu, 2014; Vijayan *et al.*, 2014). The average particle size of biosynthesized NS-AuNPs by using Debye-Scherrer equation were found to be around  $22\text{ nm}$  and crystallinity was found to be  $27\%$  for NS- AuNPs. FT-IR analysis verified the interaction of different functional groups on the AuNPs surface (Figure 4) of *A. indica* seed and their as-synthesized AuNPs. Analysis of the FT-IR spectra of *A. indica* seed showed the presence of various peaks at  $3325$ ,  $2946$ ,  $2834$ ,  $1652$ ,  $1449$ ,  $1412$ ,  $1112$  and  $1017\text{ cm}^{-1}$  and their NS-AuNPs also presented peaks at  $3337$ ,  $2924$ ,  $2853$ ,  $1646$ ,  $1409$  and  $1016\text{ cm}^{-1}$ , respectively (Gatea *et al.*, 2015; Elia *et al.*, 2014). The similarity of these two spectra, along with a slight shift in peak positions, demonstrated that the different groups from the *A. indica* seed were capped with the AuNPs (Foo *et al.*, 2017).

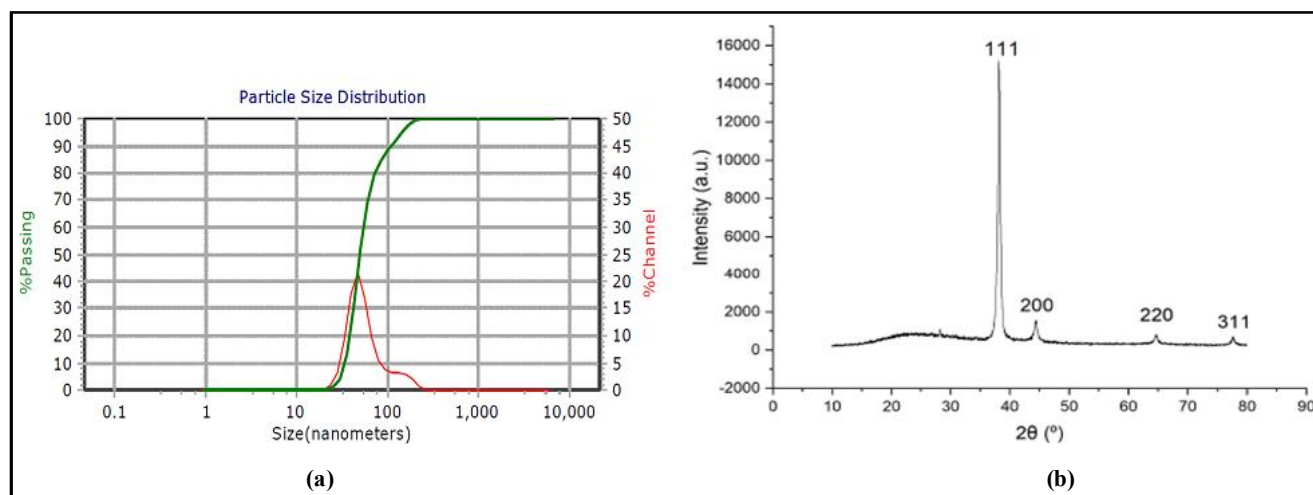


Figure 3: Particle size distribution (a) and XRD patterns (b) of biosynthesized NS-AuNPs.

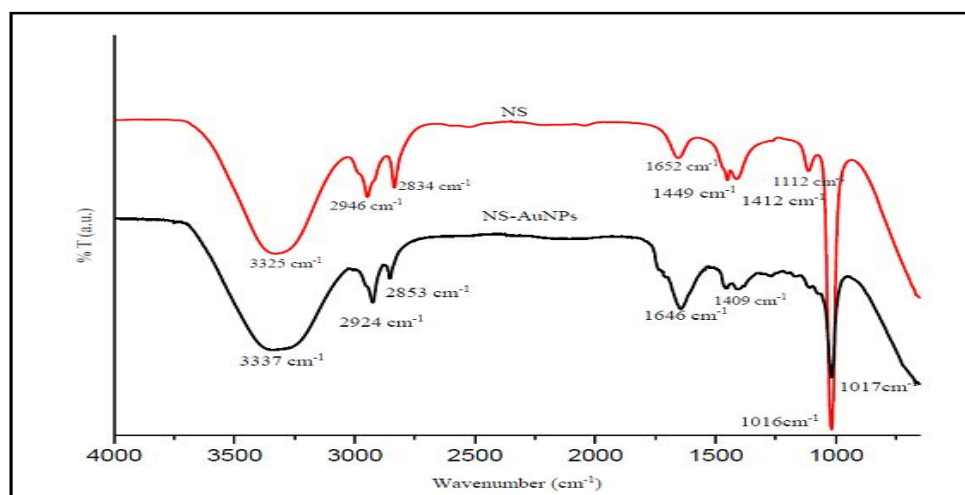
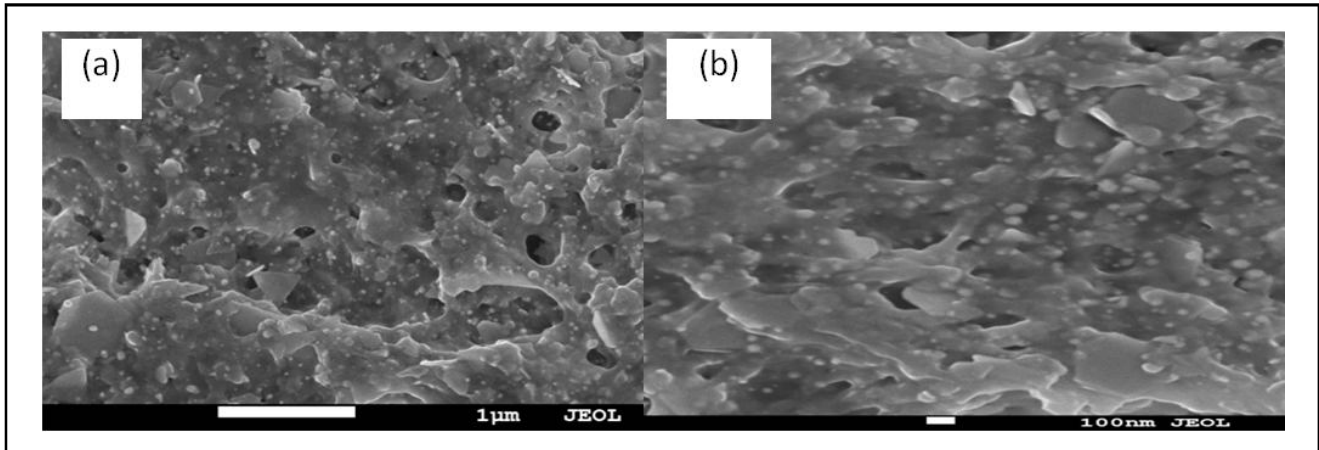


Figure 4: Comparative FT-IR spectra of *A. indica* seed and their biosynthesized AuNPs.

It was discovered that most biosynthesised AuNPs were spherical, with some having rod and triangular shapes. Small and large sized NPs coexisted because of the variation in their formation over time during synthesis, indicating that the aggregation and formation of

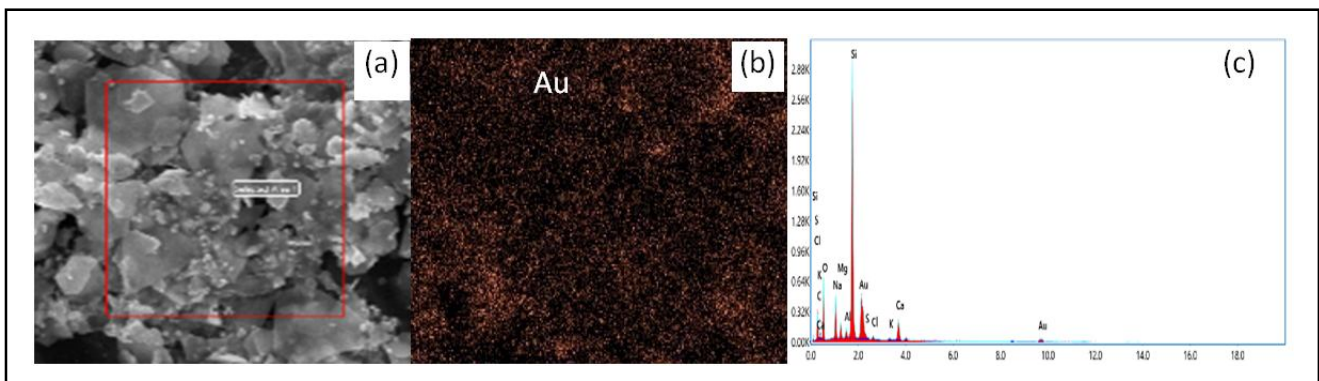
new NPs happened at the same time (Figure 5). More than 50 NPs were analyzed for size distribution by using Image J software (Gangula *et al.*, 2011). The average diameter of the *A. indica* seed AuNPs was found to be 23 nm, and their sizes ranged from 15 to 31 nm.



**Figure 5:** FESEM micrographic images of NS-AuNPs at different magnification level (a) 1  $\mu\text{m}$ , (b) 100 nm.

In the case of NS-AuNPs (Figure 6), the strong optical absorption peak at 2.1 and 9.6 Kev confirmed the presence of metallic gold (Au) (Wang *et al.*, 2016; Dauthal and Mukhopadhyay, 2013). The analysis of NS-AuNPs using energy dispersive X-ray spectroscopy (EDX)

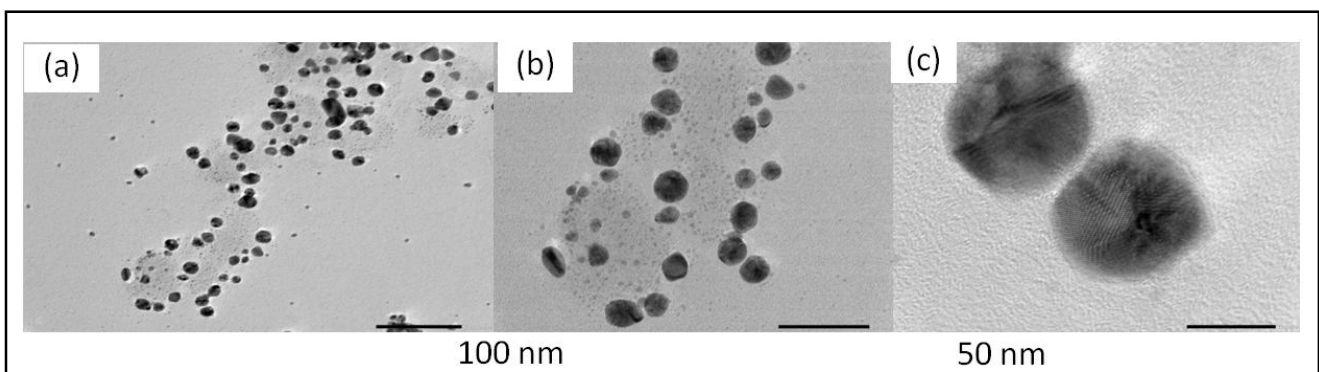
verified the existence of metallic gold (35.71%), carbon (17.10%), and oxygen (21.42%). Elemental mapping was also done during FESEM analysis which confirmed the presence of elementary Au in the biosynthesized NS-AuNPs.



**Figure 6:** (a) EDX analysis, (b) showing presence of Au in the sample and (c) elemental analysis of the selected area of NS-AuNPs.

Images captured by HRTEM reveal that the majority of biosynthesised NS-AuNPs were spherical, though some were occasionally triangular and rod-shaped. The biosynthesized AuNPs were mainly monodispersed with diameter ranging from 3 to 28 nm (Figure 7) with average diameter of 13 nm. The reflections of FCC

gold identified by the diffraction ring obtained from the inner to the outer selected area electron diffraction (SAED) image are (111), (200), and (220), which are in good agreement with the information derived from XRD analysis (Vijayan *et al.*, 2014).



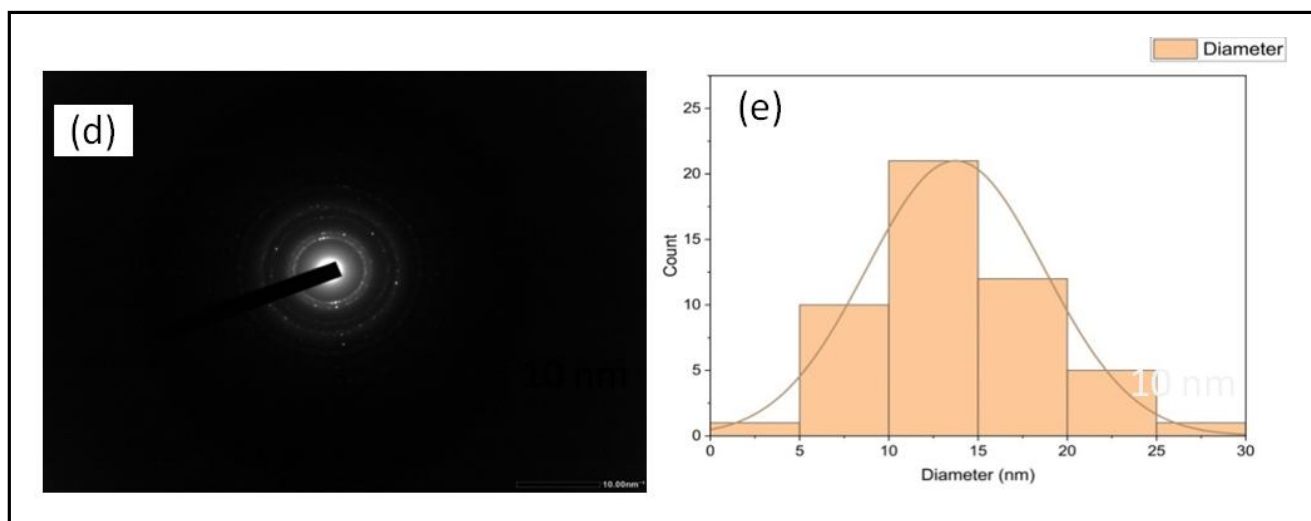


**Figure 7:** Images of HRTEM showing the presence of NPs of *A. indica* seed recorded at different magnification level (a-c), SAED pattern (d), histogram showing distribution of size of NPs (e).

### 3.4 Evaluation of antioxidant activity

#### 3.4.1 Evaluation and comparison of antioxidant activity of biosynthesized AuNPs of *A. indica* seed aqueous extract by DPPH free radical scavenging activity method

DPPH free radical scavenging activity of biosynthesized AuNPs of *A. indica* seed varied widely and showed direct relation with

concentration levels (Table 1). Quadratic equation for estimating  $IC_{50}$  value was calculated by plotting graph between extract concentration and DPPH free radical scavenging activity (%) of NS-AuNPs. The  $IC_{50}$  value of 83 and 71.75 ppm was obtained for NS-AuNPs and *A. indica* seed, respectively. Antioxidant activity of plant extract (*Costus pictus*) was found to be higher than biosynthesized AuNPs of same plant extract (Nakkala *et al.*, 2015).

**Table 1:** Comparative DPPH free radical scavenging activity (%) of biosynthesized NS-AuNPs with their respective aqueous extract

S. No.	Conc. (ppm)	DPPH free radical scavenging activity (%)						$IC_{50}$ (ppm)
		180	150	120	90	60	30	
1.	NS extract	74.1	70.1	64.3	56.7	45.4	21.9	71.75
2.	NS-AuNPs extract	69.3	62.8	57.9	50.2	39.3	17.1	83

**Table 2:** Comparative total antioxidant activity (%) of biosynthesized NS-AuNPs with their respective aqueous extract

S. No.	Conc. (ppm)	Total antioxidant activity (%)						$IC_{50}$ (ppm)
		180	150	120	90	60	30	
1.	NS extract	71.8	65.1	59.6	51.7	41.4	18.6	87.75
2.	NS-AuNPs extract	64.9	57.4	51.2	43.8	32.6	14.9	99.5

#### 3.4.2 Evaluation and comparison of total antioxidant activity of biosynthesized AuNPs of *A. indica* seed aqueous extract by phosphomolybdenum method

Variation in total antioxidant activity of biosynthesized AuNPs of *A. indica* seed was observed and showed direct relation with concentration levels (Table 2).

Quadratic regression equation for estimating  $IC_{50}$  value was calculated by plotting graph between total antioxidant activity (%) of NS-AuNPs and extract concentration. The  $IC_{50}$  value of 87.75 and 99.5 ppm was obtained for *A. indica* seed and NS-AuNPs, respectively. Adewale *et al.*, (2020) evaluated that with respect to Ascorbic acid, AuNPs demonstrated less antioxidant activity than crude extract.

#### 3.5 Evaluation of catalytic activity of *A. indica* seed extracts biosynthesized AuNPs

*A. indica* seed extract biosynthesised colloidal AuNPs were added to the reaction mixture, and as a result, the absorption peak at 402 nm rapidly decreased and a new peak at 305.2 nm simultaneously formed (Figure 8), indicating the formation of 4-aminophenol (Yuan *et al.*, 2017; Srinath and Rai, 2015).

Since the concentration of  $BH_4^-$  was significantly higher than that of 4-NP, pseudo first-order rate kinetics can be applied to the reduction reaction (Figure 9). The catalytic rate constant (k) was determined to be  $0.103 \text{ min}^{-1}$  by utilising the UV-Vis data (Jang *et al.*, 2020).

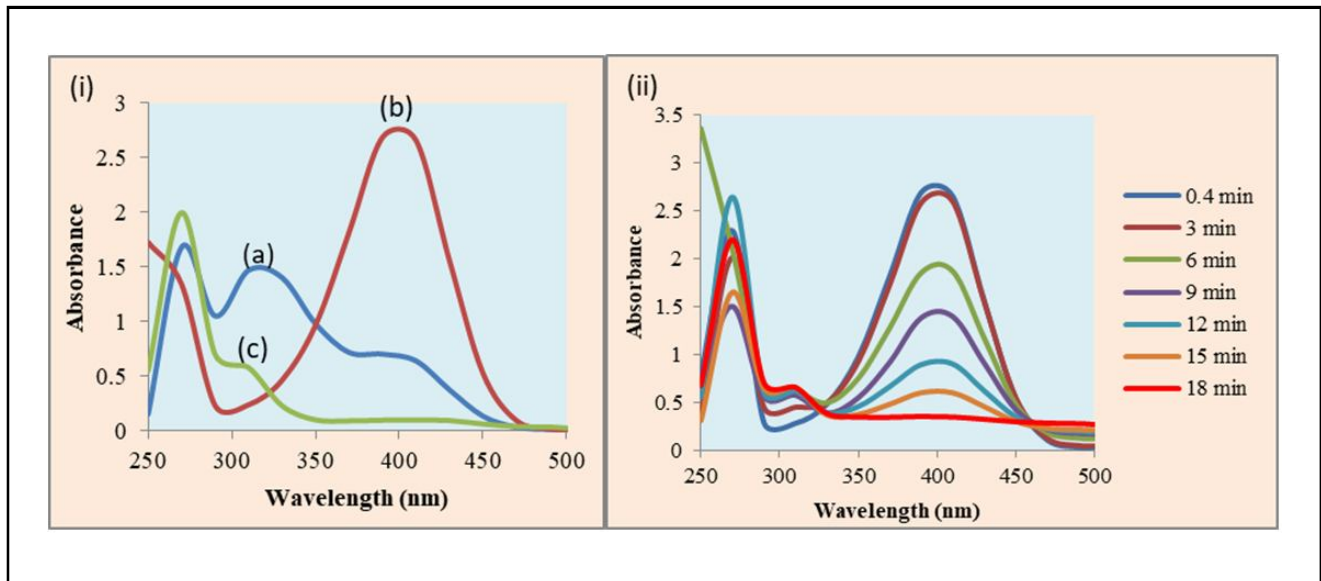


**Figure 8:** (i) UV-Vis spectrum showing complete reduction of 4-NP to 4-aminophenol of NS-AuNPs: (a) 4-NP (0.01 M), (b) 4-NP (0.01 M) in the presence of  $\text{NaBH}_4$  (0.1 M), (c) after addition of catalytic AuNPs in reaction mixture (20 min) (ii) UV-Vis spectrum of NS-AuNPs showing the progress of reduction reaction at regular time interval.

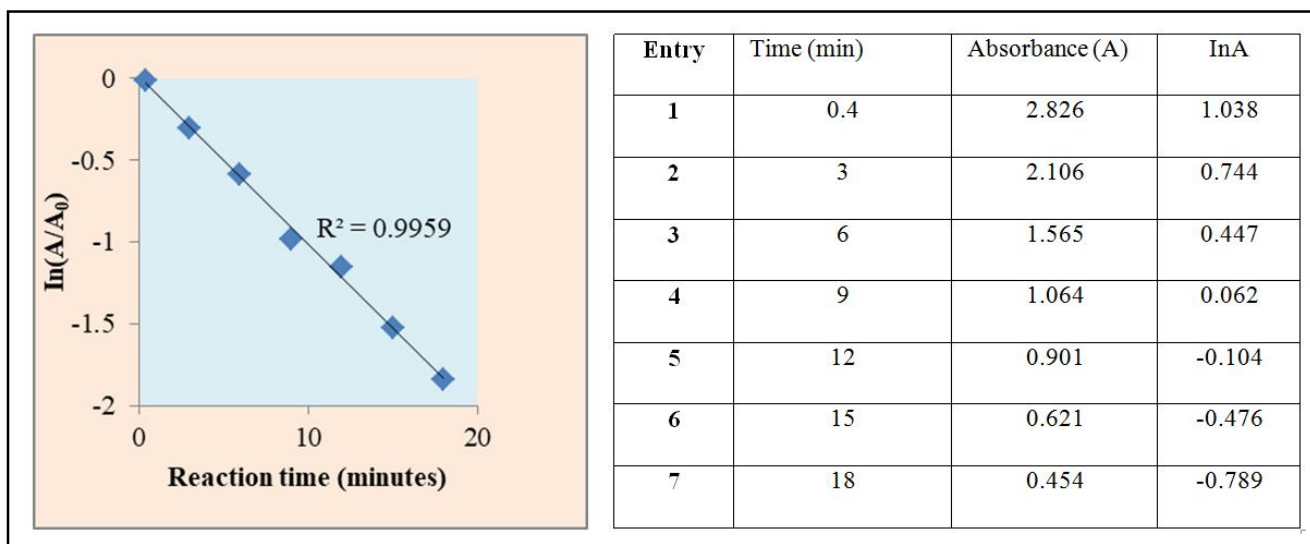


**Figure 9:** Plot of  $\ln(A/A_0)$  versus time of the NS-AuNPs, table showing the absorbance of 4-nitrophenolate ion at regular time interval for NS-AuNPs.

### 3.6 Evaluation of antimicrobial activity

Using an aqueous extract (40  $\mu\text{g/ml}$ ) of *A. indica* seed and biosynthesized AuNPs, the antimicrobial activity against various strains of bacteria and fungi, such as *Xanthomonas* spp., *S. aureus*, *Fusarium oxysporum*, and *Macrophomina phaseolina* was assessed by measuring the growth or diameter of the zone of inhibition (mm).

#### 3.6.1 Evaluation of antibacterial activity of aqueous *A. indica* seed extract as well as biosynthesized AuNPs

Aqueous extracts (40  $\mu\text{g/ml}$ ) of *A. indica* seed and their biosynthesized AuNPs showed effective zone of inhibition (Figure 10) as compared to standard antibiotic (Streptomycin) at a concentration of 15  $\mu\text{g/ml}$  for Gram-negative and Gram-positive bacteria (Table 3)

(Joe *et al.*, 2017; Girish *et al.*, 2018). Zone of inhibition was found to be maximum for biosynthesized AuNPs (20.5 mm), followed by *A. indica* seed (16.5 mm) against *S. aureus*. Similarly, order of zone of inhibition was found to be maximum for biosynthesized AuNPs (18 mm), followed by *A. indica* seed (15.5 mm) against *Xanthomonas* spp.

#### 3.6.2 Evaluation of antifungal activity of aqueous *A. indica* seed extract as well as biosynthesized AuNPs

Aqueous extracts (40  $\mu\text{g/ml}$ ) of *A. indica* seed and their biosynthesized AuNPs showed effective zone of inhibition (Figure 11) as compared to standard antibiotic (Nystatin) at a concentration of 20  $\mu\text{g/ml}$  for *M. phaseolina* and *F. oxysporum*, respectively (Table 4). Order of zone of inhibition was found to be maximum for *A. indica* seed (15.5

mm), followed by biosynthesized AuNPs (14 mm) against *M. phaseolina*. Similarly, order of zone of inhibition against *F. oxysporum*

was found to be maximum for *A. indica* seed (19.5 mm), followed by biosynthesized AuNPs (12.5 mm).

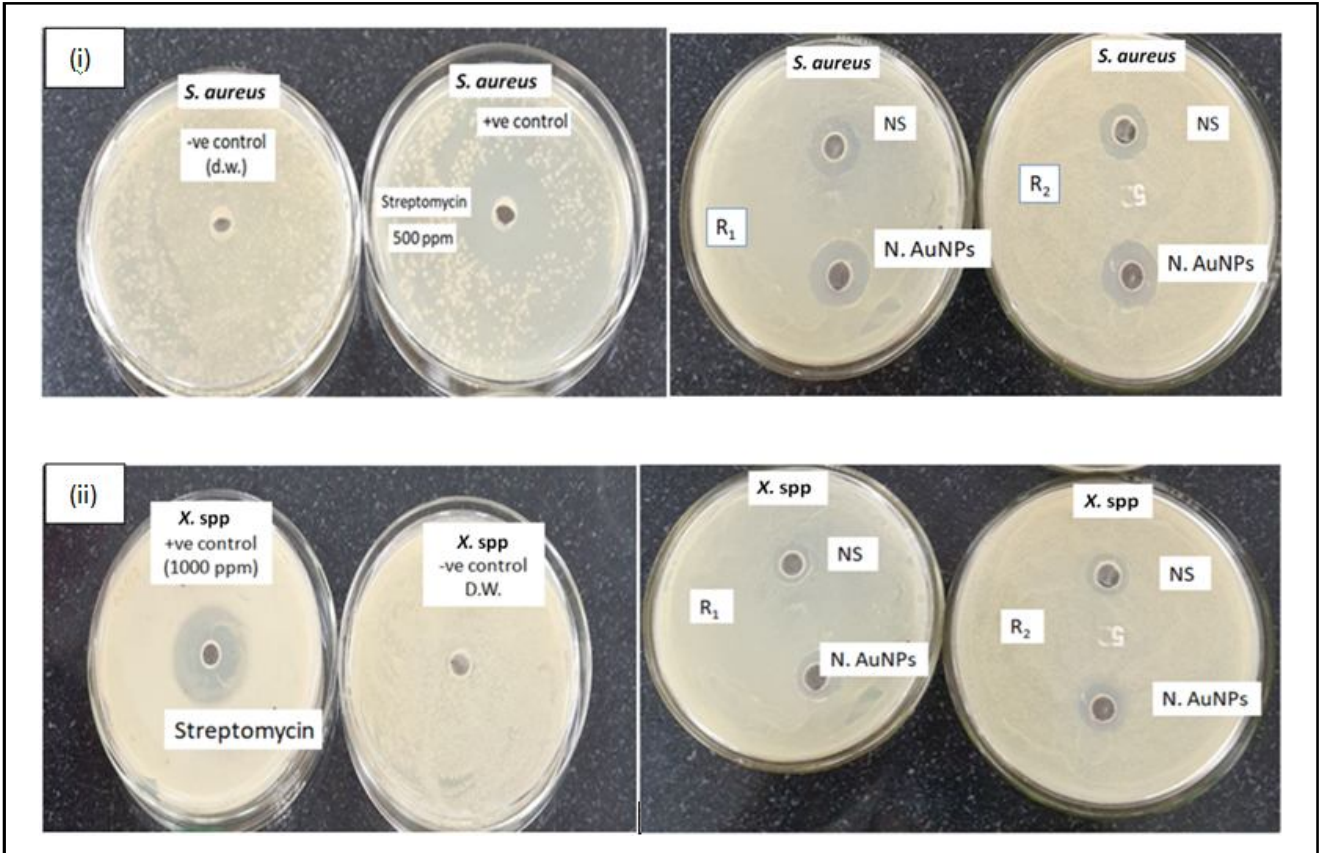


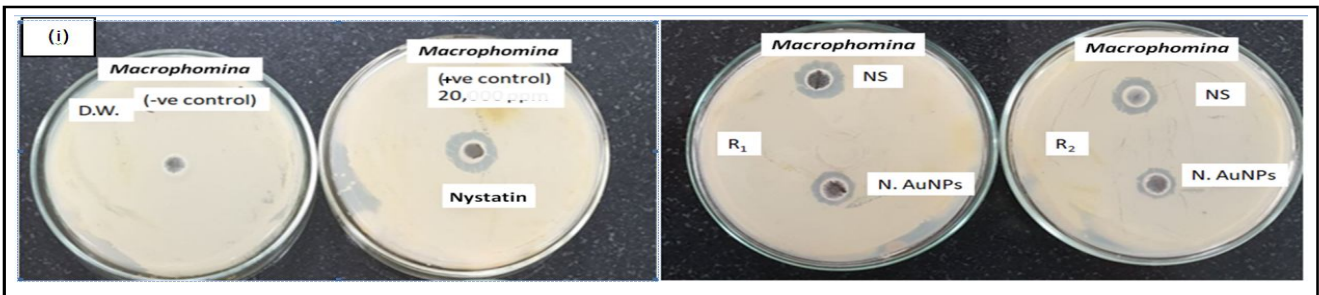
Figure 10: Image of culture plates showing antibacterial activity of *A. indica* seed and biosynthesized AuNPs against (i) *S. aureus*, (ii) *Xanthomonas* spp.

Table 3: Zone of inhibition (mm) shown against bacterial strain

Bacterial strain	Standard antibiotic Streptomycin (15 µg/ml)	<i>A. indica</i> seed	NS-AuNPs
		Zone of inhibition (mm)	
<i>S. aureus</i>	35 mm	16.5	20.5
<i>Xanthomonas</i> spp.	31 mm	15.5	18

Table 4: Zone of inhibition (mm) shown against fungal strain

Fungal strain	Standard antibiotic Nystatin (20 µg/ml)	<i>A. indica</i> seed	NS-AuNPs
		Zone of inhibition (mm)	
<i>Macrophomina phaseolina</i>	20 mm	15.5	14
<i>Fusarium oxysporum</i>	35 mm	19.5	12.5



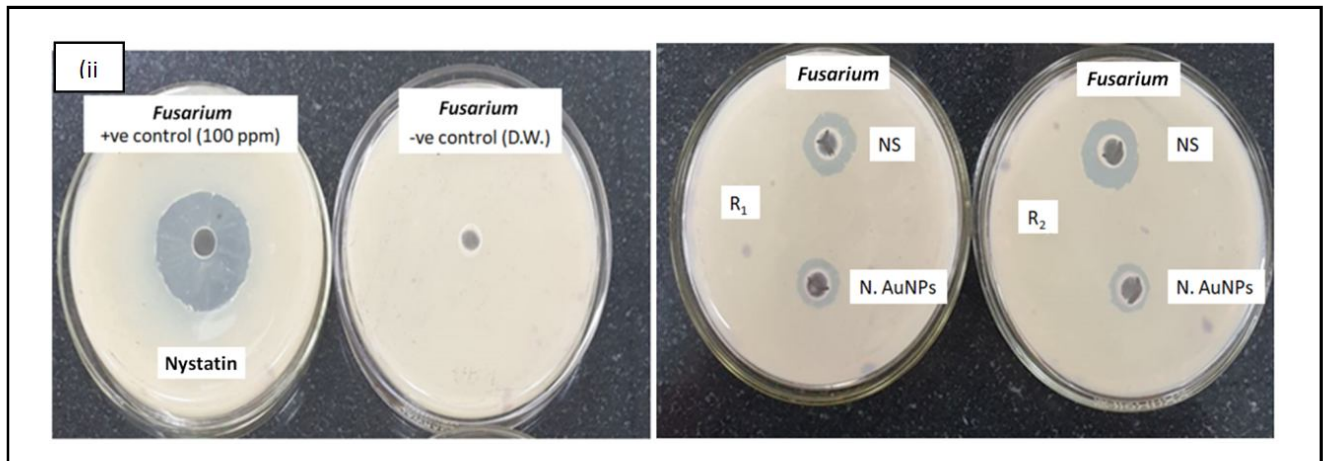


**Figure 11:** Image of culture plates showing antifungal activity of *A. indica* seed and biosynthesized AuNPs against (i) *Macrophomina phaseolina*, (ii) *Fusarium oxysporum*.

#### 4. Discussion

Using *A. indica* seed extract, several physicochemical parameters such as plant extract concentration, gold salt concentration, pH, temperature, and reaction duration were tuned for the biosynthesis of AuNPs. The result of different concentrations of *A. indica* seed extract demonstrated that a small amount of plant extract can reduce gold ion ( $\text{Au}^{+3}$ ), but aggregation of NPs was also detected due to the low concentration of biomolecules in the extract that act as a capping agent (Emmanuel *et al.*, 2014). With a rise in extract concentration, the maximum absorbance (max) of the SPR band increased, but there was also an increase in reducing agent, which interacts with the capping agent of already reduced nanoparticles on the surface of NPs, resulting in particle size increase (Gangula *et al.*, 2011).

The interaction of oscillation of electrons existing on the surface of AuNPs and incident light wave from spectrophotometer produces surface plasmon resonance (SPR) of biosynthesized AuNPs. The band width and spectrum position of SPR are affected by the size, shape, dielectric constant, and various functional groups adsorbed on the surface of NPs (Vigneshwaran *et al.*, 2007). Particle size analyzers are characterization tools that are used to determine the size, zeta potential, size distribution profile, and polydispersity index of nanoparticles in colloidal suspensions. Using dynamic light scattering, the average hydrodynamic diameter of biosynthesized AuNPs made from *Salvia officinalis*, *Pelargonium graveolens*, *Lippia citriodora*, and *Punica granatum* extract was found to be around 72, 78, 50, and 312 nm, respectively (Elia *et al.*, 2014). The extract was analyzed using FT-IR spectrum analysis to determine which functional groups are responsible for the stability and capping of biosynthesized AuNPs. Both the extract and the biosynthesized AuNPs were subjected to a comparative study. The existence of the identical chemicals in both reaction mediums was revealed by the high resemblance in peak position between biosynthesized AuNPs and extract (Dash and Bag, 2014; Umamaheswari *et al.*, 2018). The observed Bragg's reflection matching to the diffraction angles of gold's face centered cubic (FCC) acquired from XRD analysis was compared to the previously published standard (JCPDS no. 04-0784). The average particle size of AuNPs produced from *Hibiscus rosa-sinensis* was calculated using the most intense peak or peak of predominant orientation, which was determined to be 13nm (Philip,

2010). FESEM combined with EDX method and elemental mapping were used to investigate the surface shape, chemical composition and purity of biosynthesized AuNPs made from *A. indica* seed. NS-AuNPs were found to have an average diameter of 23 nm and a size range of 15-31 nm (Bankar *et al.*, 2010). The shape, size, and crystallinity of biosynthesized AuNPs were determined using the HRTEM with SAED pattern. In NL-AuNPs and NS-AuNPs, the presence of an FCC lattice of metallic gold with triangular, spherical, and rod shaped AuNPs with average diameters of 9 and 13 nm was discovered (Dash and Bag, 2014; Ahmad *et al.*, 2015).

The antioxidant activity of *A. indica* seed was significantly increased by extracting solvents utilised for phytochemicals, primarily phenolic components. The presence of antioxidants as a proton donor lowered DPPH solutions in the presence of antioxidants (Koleva *et al.*, 2002; Rice-Evans *et al.*, 1997) stated that phenolic compounds are recognised to be strong antioxidants due to their unique structural chemistry. In comparison to aqueous and acetone extracts, the methanol extract had the highest total flavanoids and phenols in the current investigation on *A. indica* seed extract. The antioxidant activity of total phenolics and flavanoids is directly connected to their ability to protect against free radicals (Ghasemzadeh *et al.*, 2010). Chahardoli *et al.* (2018) used *Nigella arvensis* leaf extract (NA-AuNPs) to biosynthesize AuNPs and tested their antioxidant efficacy at concentrations extending from 100 to 500 ppm. The antioxidant activity of plant extract (32%) was found to be higher than that of NA-AuNPs (12%) at the highest concentration (500 ppm).

Because of their biocompatibility, easy-to-control morphological traits, and great stability, AuNPs stand out among metallic nanoparticles in terms of catalytic properties (Jang *et al.*, 2020). By adding 40  $\mu\text{l}$  of NS-AuNPs to a reaction mixture containing a freshly prepared solution of 4-nitrophenol and  $\text{NaBH}_4$ , 4-nitrophenol was reduced to 4-aminophenol. The rate constant found in our investigation was equivalent to the recently published value ( $0.22 \text{ min}^{-1}$ ) of biosynthesized AuNPs utilising *Punica granatum* juice extract, according to a previous work (Dash and Bag, 2014).

Metallic nanoparticles are extremely important and widely employed in biological and engineering research. Because of their antibacterial effectiveness against infections, nanoparticles can be employed instead of standard antibiotics to overcome bacterial resistance

(Sánchez-Lopez *et al.*, 2020). The antibacterial activity of the extract and biosynthesised AuNPs had greater antibacterial activity against Gram-positive bacteria than Gram-negative bacteria, which is mainly concerned with the bacteria's cell wall composition. Metal ions are slowly released from metal nanoparticles and pass through the cell membrane, where they interact with the functional groups of enzymes, proteins, lipids, and nucleic acids, such as the -NH, -SH, and -COOH groups, they cause morphological changes and inhibit enzymatic activity (Figure 12). The respiratory system is hampered

by the irreversible alteration in membrane permeability that results from changing or the formation of non-uniform pits on the cell wall (Wang *et al.*, 2017). Previous research has found that the surface charges of AuNPs and the electric characteristics of the phospholipid bilayer have the greatest impact on NP adsorption to membranes (Lin *et al.*, 2010). Antibacterial activity of aqueous extract (40 µg/ml) of *A. indica* seed and their biosynthesized AuNPs were assessed against gram positive (*S. aureus*) and gram negative (*Xanthomonas spp.*) bacteria. In comparison to *A. indica* seed, the maximum zone of inhibition was discovered for biosynthesised AuNPs.

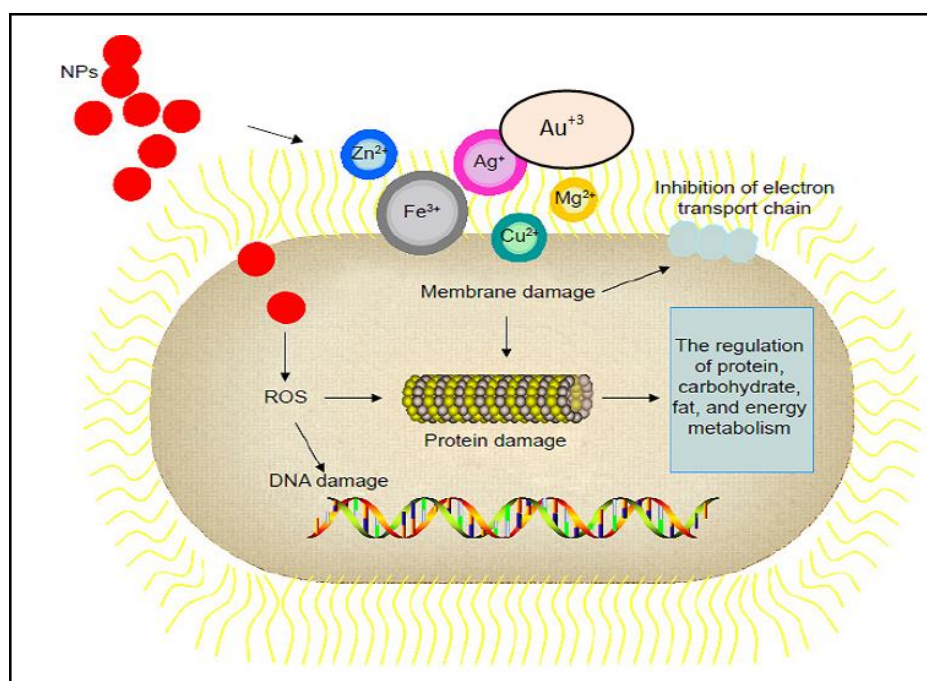


**Figure 12: Mechanism of action of antimicrobial activity of nanoparticles (Linlin Wang, 2017).**

Against *Macrophomina phaseolina* and *Fusarium oxysporum*, the antifungal activity of aqueous extract (40 g/ml) of *A. indica* seed and their biosynthesized AuNPs was tested. Antifungal activity of aqueous extract (40 µg/ml) of *A. indica* seed and their biosynthesized AuNPs were evaluated against *Fusarium oxysporum* and *Macrophomina phaseolina*. The results showed that the zone of inhibition fell between 8 and 18 mm. Order of zone of inhibition was found to be maximum for *A. indica* seed as compare to biosynthesized AuNPs. Using the standard well diffusion method, the antifungal activity of biosynthesised AuNPs derived from *Abelmoschus esculentus* seed aqueous extract was evaluated against *Puccinia graministritici*, *A. flavus*, *A. niger*, and *Candida albicans*. The results showed that the zone of inhibition fell between 8 and 18 mm (Jayaseelan *et al.*, 2013). Donga *et al.* (2020) tested the antifungal activity of biosynthesized AuNPs against three fungal strains, *C. neoformans*, *C. albicans*, and *C. glabrata*, using *Mangifera indica* seed aqueous extract, and found *C. glabrata* to be the most resistant.

## 5. Conclusion

Gold nanoparticles (AuNPs) were efficiently biosynthesized using *Azadirachta indica* seed extract, offering a low-cost, eco-friendly method without the need for reducing or stabilizing agents. The resulting nanoparticles, sized between 10 and 25 nm, exhibited strong

antioxidant, antimicrobial, and catalytic activities. Characterization confirmed their surface plasmon resonance and effective role in reducing 4-nitrophenol. This green synthesis method demonstrates significant biological and catalytic potential.

## Acknowledgments

The authors thank Dr. R. S. Dhillon, Department of Forestry of Chaudhary Charan Singh Haryana Agricultural University, Hisar for the procurement of Seeds of *A. indica*. The authors also thank Department of Chemistry, CCS Haryana Agricultural University, Hisar, Haryana, India for providing excellent research facilities.

## Conflict of interest

The authors declare no conflicts of interest relevant to this article.

## References

- Adewale, O.B.; Egberemi, K.A.; Onwuelu, J.O.; Potts-Johnson, S.S.; Anadozie, S.O.; Fadaka, A. O.; Osukoya, O.A.; Aluko, B.T.; Johnson, J.; Obafemi, T.O. and Onasanya, A. (2020). Biological synthesis of gold and silver nanoparticles using leaf extracts of *Crassocephalum rubens* and their comparative *in vitro* antioxidant activities. *Heliyon*, 6(11):e05501.
- Aggarwal, P.; Singh, S.; Sangwan, S.; Moond, M. and Devi, P. (2022). Effect of extraction solvents on antioxidant potential of *Prosopis cineraria* (L.) leaves. *Ann. Phytomed.*, 11(1):426-431.

- Ahmad, A.; Wei, Y.; Syed, F.; Imran, M.; Khan, Z.U.H.; Tahir, K. and Yuan, Q. (2015). Size dependent catalytic activities of green synthesized gold nanoparticles and electro-catalytic oxidation of catechol on gold nanoparticles modified electrode. RSC advances, **5**(120):99364-99377.
- Ahmad, T.; Irfan, M.; Bustam, M.A. and Bhattacharjee, S. (2016). Effect of reaction time on green synthesis of gold nanoparticles by using aqueous extract of *Elaise guineensis* (oil palm leaves). Procedia Engineering, **148**:467-472.
- Anastas, P. T. and Warner, J. C. (1998). Green chemistry. Frontiers, **640**, 1998.
- Anuradha, J.; Abbasi, T. and Abbasi, S.A. (2010). Green synthesis of gold nanoparticles with aqueous extracts of *A. indica* (*Azadirachta indica*). Research Journal of Biotechnology, **5**(1):75-79.
- Bankar, A.; Joshi, B.; Kumar, A. R. and Zinjarde, S. (2010). Banana peel extract mediated novel route for the synthesis of silver nanoparticles. Colloids and Surfaces A: Physicochemical and Engineering Aspects, **368**(1-3):58-63.
- Beniwal, A.; Singh, S.; Saini, K.; Rani, J.; Kakkar, S.; Moond, M. and Yogita (2023). Phytochemical analysis of acetone extract of *Cassia siamea* L. J. Phytanotech. Pharmaceut. Sci., **3**(2):1-6.
- Chahardoli, A.; Karimi, N.; Sadeghi, F. and Fattahi, A. (2018). Green approach for synthesis of gold nanoparticles from *Nigella arvensis* leaf extract and evaluation of their antibacterial, antioxidant, cytotoxicity and catalytic activities. Artificial Cells, Nanomedicine, and Biotechnology, **46**(3):579-588.
- Dalal, R.; Singh, S.; Sangwan, S.; Moond, M. and Beniwal, R. (2022). Biochemical and molecular mechanism of plant-mediated synthesis of silver nanoparticles: A review, Mini-Reviews in Organic Chemistry, **19**(8):939-954.
- Dash, S.S. and Bag, B.G. (2014). Synthesis of gold nanoparticles using renewable *Punica granatum* juice and study of its catalytic activity. Applied Nanoscience, **4**(1):55-59.
- Dauthal, P. and Mukhopadhyay, M. (2013). *In vitro* free radical scavenging activity of biosynthesized gold and silver nanoparticles using *Prunus armeniaca* (apricot) fruit extract. Journal of Nanoparticle Research, **15**(1):1-11.
- Devi, D.; Singh, S.; Moond, M.; Matoria, P.; Kumari, S.; Saini, K. and Sharma, R.K. (2023). Phytochemical analysis and antioxidant potential of *Albizia lebeck* (L.) seeds. Ann. Phytomed., **12**:502-507.
- Devi, R.; Singh, S.; Moond, M.; Beniwal, R.; Kumar, S.; Kumari, S. and Sharma, R.K. (2023). Proximate composition, phenolic-flavonoid content and antioxidant potential of *Syzygium cumini* (L.) Skeels seed powder. Ann. Phytomed., **12**(1): 508-513.
- Donga, S.; Bhadu, G. R. and Chanda, S. (2020). Antimicrobial, antioxidant and anticancer activities of gold nanoparticles green synthesized using *Mangifera indica* seed aqueous extract. Artificial Cells, Nanomedicine, and Biotechnology, **48**(1):1315-1325.
- Eid, A.; Jaradat, N. and Elmarzugi, N. (2017). A review of chemical constituents and traditional usage of *A. indica* plant (*Azadirachta indica*). Pelestinian Medical and Pharmaceutical Journal, **2**(2):75-81.
- Elia, P.; Zach, R.; Hazan, S.; Kolusheva, S.; Porat, Z.E. and Zeiri, Y. (2014). Green synthesis of gold nanoparticles using plant extracts as reducing agents. International Journal of Nanomedicine, **9**(1):4007-4021.
- Emmanuel, R.; Karupiah, C.; Chen, S. M.; Palanisamy, S.; Padmavathy, S. and Prakash, P. (2014). Green synthesis of gold nanoparticles for trace level detection of a hazardous pollutant (nitrobenzene) causing Methemoglobinemia. Journal of Hazardous Materials, **279**:117-124.
- Foo, Y. Y.; Periasamy, V.; Kiew, L. V.; Kumar, G.G. and Malek, S.N.A. (2017). Curcuma mangga-mediated synthesis of gold nanoparticles: characterization, stability, cytotoxicity, and blood compatibility. Nanomaterials, **7**(6):123.
- Gangula, A.; Podila, R.; Karanam, L.; Janardhana, C. and Rao, A. M. (2011). Catalytic reduction of 4-nitrophenol using biogenic gold and silver nanoparticles derived from *Breynia rhamnoides*. Langmuir, **27**(24):15268-15274.
- Gatea, F.; Teodor, E. D.; Seciu, A. M.; Covaci, O.I.; Mănoiu, S.; Lazăr, V. and Radu, G.L. (2015). Antitumour, antimicrobial and catalytic activity of gold nanoparticles synthesized by different pH propolis extracts. Journal of Nanoparticle Research, **17**(7):1-13.
- Ghasemzadeh, A.; Jaafar, H. Z. and Rahmat, A. (2010). Antioxidant activities, total phenolics and flavonoids content in two varieties of Malaysia young ginger (*Zingiber officinale* Roscoe). Molecules, **15**(6):4324-4333.
- Ghoreishi, S.M.; Behpour, M. and Khayatkashani, M. (2011). Green synthesis of silver and gold nanoparticles using *Rosa damascena* and its primary application in electrochemistry. Physica E: Low-Dimensional Systems and Nanostructures, **44**(1):97-104.
- Girish, K. (2018). *A. indica* (*Azadirachta indica* A. Juss) as a source for green synthesis of nanoparticles. Asian J. Pharm. Clin. Res., **11**(3):15.
- Gopalakrishnan, R. and Raghun, K. (2014). Biosynthesis and characterization of gold and silver nanoparticles using milk thistle (*Silybum marianum*) seed extract. Journal of Nanoscience, **1**:1-8.
- Hatano, T.; Kagawa, H.; Yasuhara, T. and Okuda, T. (1988). Two new flavonoids and other constituents in licorice root, their relative astringency and radical scavenging effects. Chemical and Pharmaceutical Bulletin, **36**:2090-2097.
- Ismail, E.H.; Khalil, M. M.; Al Seif, F.A.; El-Magdoub, F.; Bent, A. N.; Rahman, A.; and Al, U.S. D. (2014). Biosynthesis of gold nanoparticles using extract of grape (*Vitis vinifera*) leaves and seeds. Progress in Nanotechnology and Nanomaterials, **3**:1-12.
- Jang, W.; Yun, J.; Ludwig, L.; Jang, S. G.; Bae, J. Y.; Byun, H. and Kim, J. H. (2020). Comparative catalytic properties of supported and encapsulated gold nanoparticles in homocoupling reactions. Frontiers in Chemistry, **8**:834.
- Jayaseelan, C.; Ramkumar, R.; Rahuman, A.A. and Perumal, P. (2013). Green synthesis of gold nanoparticles using seed aqueous extract of *Abelmoschus esculentus* and its antifungal activity. Industrial Crops and Products, **45**:423-429.
- Joe, M.H.; Jeong, H.T.; Lee, H.M.; Park, H.J.; Kim, D.H.; Park, D.H. and Bai, S. (2017). Phytosynthesis of silver and gold nanoparticles using the hot water extract of mixed woodchip powder and their antibacterial efficacy. Journal of Nanomaterials, Review, pp:221.
- Khan, M.Z.H.; Tareq, F.K.; Hossen, M.A. and Roki, M.N.A.M. (2018). Green synthesis and characterization of silver nanoparticles using *Coriandrum sativum* leaf extract. J. Eng. Sci. Technol., **13**:158-166.
- Koleva, I.I.; Van Beek, T.A.; Linszen, J. P.; Groot, A. D. and Evtatieva, L.N. (2002). Screening of plant extracts for antioxidant activity: a comparative study on three testing methods. Phytochemical Analysis: An International Journal of Plant Chemical and Biochemical Techniques, **13**(1):8-17.
- Kumar, B.; Smita, K.; Vizuete, K.S. and Cumbal, L. (2016). Aqueous phase Lavender leaf mediated green synthesis of gold nanoparticles and evaluation of its antioxidant activity. Biology and Medicine, **8**(3):1.
- Kumar, K.P.; Paul, W.; Sharma, C.P. (2011). Green synthesis of gold nanoparticles with *Zingiber officinale* extract: Characterization and blood compatibility. Process Biochemistry, **46**(10):2007-2013.
- Lin, J.; Zhang, H.; Chen, Z. and Zheng, Y. (2010). Penetration of lipid membranes by gold nanoparticles: Insights into cellular uptake, cytotoxicity, and their relationship. ACS Nano., **4**(9):5421-5429.
- Linlin Wang; Chen Hu and Longquan Shao (2017). The antimicrobial activity of nanoparticles: Present situation and prospects for the future. International Journal of Nanomedicine, **12**:1227-249.

- Link, S. and El-Sayed, M.A. (1999). Size and temperature dependence of the plasmon absorption of colloidal gold nanoparticles. *The Journal of Physical Chemistry B*, **103**(21):4212-4217.
- Mahmoud, D.A.; Hassanein, N.M.; Youssef, K.A. and AbouZeid, M.A. (2011). Antifungal activity of different *A. indica* leaf extracts and the nimonol against some important human pathogens. *Brazilian Journal of Microbiology*, **42**(3):1007-1016.
- Moond, M.; Singh, S.; Rani, J., Beniwal, A. and Sharma, R.K. (2024). Biofabricated silver nanoparticles for catalytic degradation of toxic dyes and colorimetric sensing of Hg<sup>2+</sup>. *Chemistry Select*, **9**(31):e202401826.
- Moond, M.; Singh, S.; Sangwan, S.; Devi R. and Beniwal, R. (2022). Green synthesis and applications of silver nanoparticles: A systematic review. *AATCC Journal of Research*, **9**(6):272-285.
- Moond, M.; Singh, S.; Sangwan, S.; Devi, P.; Beniwal, A.; Rani, J.; Kumari, A. and Rani, S. (2023). Biosynthesis of silver nanoparticles utilizing leaf extract of *Trigonella foenum-graecum* L. for catalytic dyes degradation and colorimetric sensing of Fe<sup>3+</sup>/Hg<sup>2+</sup>. *Molecules*, **28**:951.
- Moond, M.; Singh, S.; Sangwan, S.; Devi, R.; Rani, J.; Beniwal, A. and Beniwal, R. (2023). Synthesis, optimization and characterization of Silver nanoparticles using aqueous seed extract of *Trigonella foenum-graecum* L. for catalytic reduction of p-nitrophenol. *Chemistry Select*, **8**(29):2365-6549.
- Moond, M.; Singh, S.; Sangwan, S.; Rani, J.; Beniwal, A.; Matoria, P.; Saini, K. and Sharma, R.K. (2023). Proximate composition, phytochemical analysis and antioxidant potency of *Trigonella foenum-graecum* L. seeds. *Ann. Phytomed.*, **12**(1):486-491.
- Moond, M.; Singh, S.; Sangwan, S.; Rani, S.; Beniwal, A.; Rani, J.; Kumari, A.; Rani, I. and Devi, P. (2023). Phytofabrication of silver nanoparticles using *Trigonella foenum-graecum* L. leaf and evaluation of its antimicrobial and antioxidant activities. *Int. J. Mol. Sci.*, **24**:3480.
- Nahak, G. and Sahu, R.K. (2011). Evaluation of antioxidant activity of flower and seed oil of *Azadirachta indica* A. juss. *Journal of Applied and Natural Science*, **3**(1):78-81.
- Nakkala, J.R.; Bhagat, E.; Suchiang, K. and Sadras, S.R. (2015). Comparative study of antioxidant and catalytic activity of silver and gold nanoparticles synthesized from *Costus pictus* leaf extract. *Journal of Materials Science and Technology*, **31**(10):986-994.
- Philip, D. (2010). Green synthesis of gold and silver nanoparticles using *Hibiscus rosa-sinensis*. *Physica E: Low-Dimensional Systems and Nanostructures*, **42**(5):1417-1424.
- Poonam; Singh, S.; Moond, M.; Sangwan, S. and Devi, P. (2023). Phytochemicals and antioxidant potential of *Andrographis paniculata* Nees. *Ann. Phytomed.*, **12**(2):769-775.
- Prashanth, G.K. and Krishnaiah, G.M. (2014). Chemical composition of the leaves of *Azadirachta indica* Linn (*A. indica*). *International Journal of Advancement in Engineering and Technology, Management and Applied Science*, **1**(3):21-31.
- Prieto, P.; Pineda, M. and Aguilar, M. (1999). Spectrophotometric quantitation of antioxidant capacity through the formation of a phosphor molybdenum complex: Specific application to the determination of vitamin E. *Analytical Biochemistry*, **269**:337-341.
- Puri, H. S. (1999). *A. indica* : the divine tree *Azadirachta indica*. CRC Press.
- Rani, J., Singh, S.; Beniwal, A.; Moond, M.; Kakkar, S.; Sangwan, S. and Sharma, R.K. (2024). Phytofabrication of silver nanoparticles using pomegranate juice extract for antioxidant, antimicrobial and cytotoxic activities. *Chemistry Select*, **9**(31):e202402068.
- Rice-Evans, C.; Miller, N. and Paganga, G. (1997). Antioxidant properties of phenolic compounds. *Trends in Plant Science*, **2**(4):152-159.
- Roy, N.; Mondal, S.; Laskar, R.A.; Basu, S.; Mandal, D. and Begum, N.A. (2010). Biogenic synthesis of Au and Ag nanoparticles by Indian propolis and its constituents. *Colloids and Surfaces B: Biointerfaces*, **76**(1):317-325.
- Sánchez-López, E.; Gomes, D.; Esteruelas, G.; Bonilla, L.; Lopez-Machado, A. L.; Galindo, R. and Souto; E.B. (2020). Metal-based nanoparticles as antimicrobial agents: An overview. *Nanomaterials*, **10**(2):292.
- Santosh kumar, J.; Rajesh kumar, S. and Venket Kumar, S. (2017). Phytoassisted synthesis, characterization and applications of gold nanoparticles: A review. *Biochemistry and Biophysics Reports*, **11**:46-57.
- Singh, S.; Sangwan, S.; Devi, P.; Sharma, P. and Moond, M. (2021). Nanotechnology for sustainable agriculture: An emerging perspective. *Journal of Nanoscience and Nanotechnology*, **21**(6):3453-3465.
- Singh, V. and Chauhan, D. (2014). Phytochemical evaluation of aqueous and ethanolic extract of *A. indica* leaves (*Azadirachta indica*). *Indo American Journal of Pharmaceutical Research*, **4**(12):5943-5948.
- Sithisarn, P.; Supabphol, R. and Gritsanapan, W. (2005). Antioxidant activity of Siamese *A. indica* tree (VP1209). *Journal of Ethnopharmacology*, **99**(1):109-112.
- Srinath, B. S. and Rai, R.V. (2015). Biosynthesis of gold nanoparticles using extracellular molecules produced by Enterobacteraerogenes and their catalytic study. *Journal of Cluster Science*, **26**(5):1483-1494.
- Subapriya, R. and Nagini, S. (2005). Medicinal properties of *A. indica* leaves: A review. *Current Medicinal Chemistry-Anti-Cancer Agents*, **5**(2): 149-156.
- Umamaheswari, C.; Lakshmanan, A. and Nagarajan, N. S. (2018). Phyto mediated synthesis, biological and catalytic activity studies of gold nanoparticles. *IET Nanobiotechnology*, **12**(2):166-174.
- Vigneshwaran, N.; Ashtaputre, N.M.; Varadarajan, P.V.; Nachane, R. P.; Paralikar, K.M. and Balasubramanya, R.H. (2007). Biological synthesis of silver nanoparticles using the fungus *Aspergillus flavus*. *Materials Letters*, **61**(6):1413-1418.
- Vijayan, S.R.; Santhiyagu, P.; Singamuthu, M.; Kumari Ahila, N.; Jayaraman, R. and Ethiraj, K. (2014). Synthesis and characterization of silver and gold nanoparticles using aqueous extract of seaweed, *Turbinaria conoides*, and their antimicrofouling activity. *The Scientific World Journal*, 2014:938272.
- Wang, C.; Singh, P.; Kim, Y.J.; Mathiyalagan, R.; Myagmarjav, D.; Wang, D.; Jin, C.G. and Yang, D.C. (2016). Characterization and antimicrobial application of biosynthesized gold and silver nanoparticles by using *Microbacterium resistens*. *Artificial Cells, Nanomedicine, and Biotechnology*, **44**(7):1714-1721.
- Wang, L.; Hu, C. and Shao, L. (2017). The antimicrobial activity of nanoparticles: Present situation and prospects for the future. *International Journal of Nanomedicine*, **12**:12-27.
- Yuan, C. G.; Huo, C.; Gui, B. and Cao, W.P. (2017). Green synthesis of gold nanoparticles using *Citrus maxima* peel extract and their catalytic/antibacterial activities. *IET Nanobiotechnology*, **11**(5):523-530.
- Zhan, G.; Huang, J.; Lin, L.; Lin, W.; Emmanuel, K. and Li, Q. (2011). Synthesis of gold nanoparticles by *Cacumen platycladi* leaf extract and its simulated solution: Toward the plant-mediated biosynthetic mechanism. *Journal of Nanoparticle Research*, **13**(10):4957-4968.
- Zhou, Y.; Lin, W.; Huang, J.; Wang, W.; Gao, Y.; Lin, L. and Du, M. (2010). Biosynthesis of gold nanoparticles by foliar broths: Roles of biocompounds and other attributes of the extracts. *Nanoscale Research Letters*, **5**(8):1351-1359.

## Citation

Rajita Beniwal, Sushila Singh, Seema Sangwan, Ritu Devi, Monika Moond, Jyoti Duhan and Kamaljeet Saini (2024). Green synthesis of gold nanoparticles using neem seed extract: Antioxidant, antimicrobial, and catalytic properties. *Ann. Phytomed.*, **13**(2):714-725. <http://dx.doi.org/10.54085/ap.2024.13.2.73>.